Multiscale Laminar Flows with Turbulentlike Properties

Lionel Rossi, J. C. Vassilicos, and Yannis Hardalupas
Imperial College London, London SW7 2AZ, United Kingdom
(Received 10 February 2006; published 2 October 2006)

By applying fractal electromagnetic force fields on a thin layer of brine, we generate steady quasi-two-dimensional laminar flows with multiscale stagnation point topology. This topology is shown to control the evolution of pair separation (Δ) statistics by imposing a turbulentlike locality based on the sizes and strain rates of hyperbolic stagnation points when the flows are fast enough, in which case $\overline{\Delta^2} \sim t^\gamma$ is a good approximation with γ close to 3. Spatially multiscale laminar flows with turbulentlike spectral and stirring properties are a new concept with potential applications in efficient and microfluidic mixing.

DOI: 10.1103/PhysRevLett.97.144501 PACS numbers: 47.27.−i, 47.85.L−

Introduction.—The rate with which pairs of points separate in phase or physical space is of central importance to dynamical systems. In turbulent flows, pairs of fluid elements (also referred to as particles here) separate algebraically [1–10]. As originally pointed out in Ref. [1], their statistics bear the imprint of the entire range of turbulent eddy scales. A theory has been developed recently which relates turbulent pair diffusion statistics to the multiscale streamline topology of the turbulence, specifically to its multiscale stagnation point structure [4–6,11,12]. This theory is based on the picture, originally conjectured in Ref. [2], that in turbulent flows, fluid element pairs travel together for long times and separate suddenly when they encounter a straining stagnation point. Recent laboratory experiments have confirmed that pairs travel together for long and separate in sudden bursts [3].

This new theory has been formulated for isotropic homogeneous turbulence and its central tenet is that stagnation points in the frame where the mean flow is zero are persistent enough on average to dominate the average separation rate of fluid element pairs. The rationale for this tenet is that pairs are subjected to a sustained exponential separation rate at persistent straining stagnation points as can occur nowhere else in the flow. The statistical persistence of these points has been established by direct numerical simulations and by theoretical argumentation [11,12]. The second important tenet of the theory is that straining stagnation points have a length-scale associated with them. Hence, the Richardson locality hypothesis that the pair separation rate is dominated by eddies of length-scale comparable to the pair's separation can be rephrased by replacing ''eddies'' with ''straining stagnation points''. This Richardson-type locality is a very broad concept because a wide range of power-law energy spectra can lead to power-law pair separation [4].

Because of the impossibility (at least by current means), to monitor and measure in the laboratory the multiscale topology of the turbulence on the fly and its instantaneous links to pair diffusion (i.e., identify most stagnation points and follow their paths while measuring their length scales and following fluid element pairs at the same time), we propose to test this new theory in bespoke multiscale flows with electromagnetically imposed turbulentlike multiscale stagnation point topology following the recent work of Ref. [13]. An important first case of such bespoke multiscale flow design is the case of the steady quasi-two-dimensional (Q2D) laminar flow. If nontrivial statistics of pair diffusion exist in such a flow they must necessarily result from the flow's multiscale stagnation point topology. Furthermore, multiscale laminar flows with turbulentlike properties are a new concept with potential applications in microfluidic and efficient mixers. Unlike chaotic advection [14], these flows are spatially multiscale. It is our purpose here to study pair diffusion statistics in such flows and investigate the relations of these statistics to the flow's multiscale stagnation point topology. It is therefore also our purpose to measure and characterize this multiscale stagnation point structure, in part by introducing a measurable definition of stagnation point length scale.

Multiscale flow and its stagnation point structure.—References [4,5] showed that, in 2D turbulent flows with an energy spectrum $E(k) \sim k^{-p}$ where $p < 3$, the multiscale streamline topology consists of cat's eyes within cat's eyes [see Fig. 1(b)] which implies a fractal-like distribution of stagnation points. Reference [6] showed that the number density n_s of stagnation points is a power-law function of the outer to inner length-scale ratio L/η, $n_s = C_s L^{-d}(L/\eta)^{Ds}$ where the fractal dimension D_s is such that $p + 2D_s/d = 3$ and $d = 2, 3$ for 2D, 3D turbulence. Reference [13] generated a Q2D multiscale laminar flow with an imposed multiscale spatial distribution of stagnation points and corroborated that such a flow has a power-law energy spectrum in agreement with $p + D_s = 3$. The same rig and family of flows ($p \approx 2.5$) are used here.

Experimental set-up and flow.—Figure 1(a) is a schematic of the rig. An horizontal shallow layer of brine (NaCl, 158 g/l, thickness $H = 5$ mm) is forced by a fractal distribution of opposite pairs of Lorentz forces as shown in Fig. 1(c). These electromagnetic (EM) forces are generated by an electric current through the brine and permanent magnets of various horizontal sizes (10, 40, 160 mm) placed under the bottom wall which supports the brine.

The two-component velocity field $\mathbf{u}(\mathbf{x}, t)$ at the free surface of the brine layer generated by these fractal EM

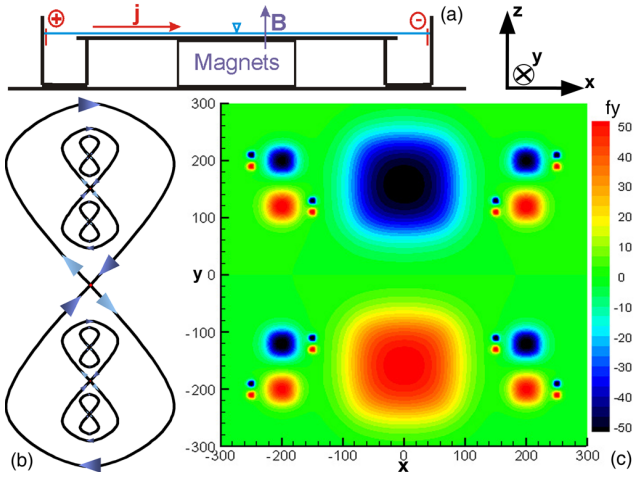

FIG. 1 (color online). (a) Schematic of rig; (b) Schematic of multiscale flow based on an 8 in 8 topology, (c) Electromagnetic forcing distribution computed for our spatial distribution of multisized magnets ($I = 1$ A, $B = 1$ T; f_y in N/m^3; x and y in mm).

forces has been measured by particle image velocimetry (PIV), using a 15 Hz, 12 bit, 2048×2048 pixel^2 camera. The flow is measured in a large square frame (which cover all magnets) of size $L_{\mathrm{PIV}} = 813.4$ mm which is small compared to the size of the tank (1700×1700 mm^2). The physical length of one pixel is about 0.3972 mm. The correlation windows have 16×16 pixels (search window 42×42 pixels), and the overlap in each direction is of 9 pixels. This leads to a measurement grid containing 287×287 velocity vectors. For full details on the rig and experiments, see Rossi *et al.* [13] who also show that the flow at the free surface of the brine is Q2D.

With steady EM forces the flows are stationary after an initial transient following the sudden switch-on of the forces. A Reynolds number $\mathrm{Re}_{2\mathrm{D}} = u_{\mathrm{rms}} L_{\mathrm{PIV}}/\nu$ is defined based on L_{PIV}, the root mean square of the PIV velocity field, u_{rms}, (which is controlled by varying the intensity of the electric current), and the kinematic viscosity of the brine, ν. In this Letter we present results obtained for 11 different values of $\mathrm{Re}_{2\mathrm{D}}$ from 600 to 9900. Even though the values of $\mathrm{Re}_{2\mathrm{D}}$ are large, all these flows are Q2D as shown in Ref. [13] and laminar as they present no instabilities and the fluid velocity values are never larger than a few cm/s.

The velocity fields are very similar over the entire range of Reynolds numbers. Indeed, the spatial correlation between two velocity fields $\mathbf{u}_1$ and $\mathbf{u}_2$ obtained at two different Reynolds numbers is always larger than 0.84 with an average of 0.947 and a standard deviation of 4.5%. Integral length scales, L_E, are obtained from the spatial autocorrelation of the velocity fields and their values slowly increase from about 16 cm to about 20 cm as $\mathrm{Re}_{2\mathrm{D}}$ increases from 600 to 9900. This increase of L_E reflects the slight increase of the largest eddy size.

Multiscale stagnation point structure.—The stagnation point positions, $\mathbf{x}_s$, are obtained with a Newton-Raphson algorithm applied to the PIV velocity field, see Fig. 2(a). The flow being incompressible, stagnation points are characterized by a single positive strain or rotation rate, λ (in 1/s), which is an eigenvalue of $J_{ij} = \partial u_i/\partial x_j$ at the stagnation point: the eigenvalues and eigenvectors $\mathbf{X}$ are given by $\mathbf{JX} = \pm\lambda\mathbf{X}$ for hyperbolic stagnation points or $\mathbf{JX} = \pm\mathbf{i}\lambda\mathbf{X}$ for elliptic ones.

Hyperbolic stagnation points also have an associated length scale L_s which, in 2D incompressible flow, scales with the size of the streamlines emanating from or passing very close to them. To define and calculate L_s we integrate the velocity $\mathbf{u}$ (obtained from our PIV and Lagrange interpolation within the PIV grid) along a streamline starting from a point $\mathbf{x}_s + \epsilon\mathbf{e}_\theta$ very close to a hyperbolic stagnation point $\mathbf{x}_s$ (ϵ is very small, within the size of the PIV grid) and $\mathbf{e}_\theta$ is a unit vector of angle θ. We track the value of $\mathbf{u} \cdot \mathbf{e}_\theta$ while integrating along the streamline and record the point $\mathbf{x}_l(\theta)$ where this quantity changes sign. We then define $L_s \equiv \langle|\mathbf{x}_l(\theta) - \mathbf{x}_s|\rangle_\theta$, where the averaging operation $\langle\ldots\rangle_\theta$ is over θ. L_s is a measure of the characteristic distance from $\mathbf{x}_s$ where streamlines passing very close to $\mathbf{x}_s$ take a turn.

We calculated L_s for all the hyperbolic stagnation points at various values of $\mathrm{Re}_{2\mathrm{D}}$. Figure 2(b) is a scatter plot of the strain rates λ and the stagnation point sizes L_s for all hyperbolic points and five different values of $\mathrm{Re}_{2\mathrm{D}}$. The hyperbolic stagnation points directly imposed by the EM forcing between the magnets [which correspond with stagnation points of the forcing; see Figs. 1(b) and 2(a)] are

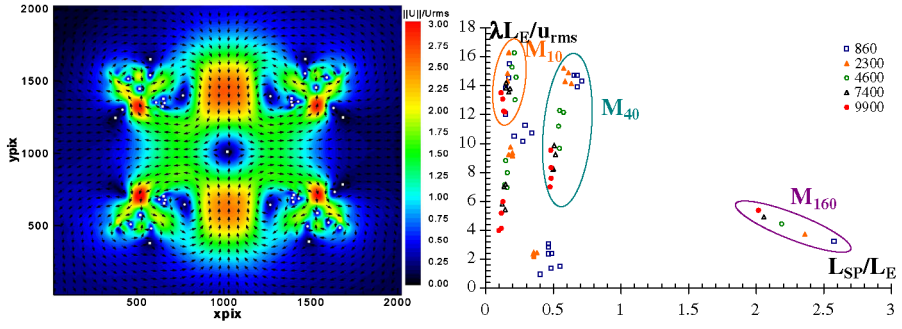

FIG. 2 (color online). (a) PIV velocity field ($\mathbf{u}/\mathbf{u}_{\mathrm{rms}}$, 1/64 arrows), $\mathrm{Re}_{2\mathrm{D}} = 600$, squares refer to hyperbolic stagnation points, disks to elliptic stagnation points; (b) scatter plot of hyperbolic stagnation point strain rates, $\lambda L_E/u_{\mathrm{rms}}$, and sizes, L_S/L_E.

circled and marked with the corresponding scale of forcing: M_{10}, M_{40}, M_{160}. It is found that the length scales L_s cluster around three values L_{s3}, L_{s2}, and L_{s1} separated by an approximate factor 4 from each other. This factor corresponds to the ratio 4 between the different magnet sizes.

In Fig. 3 we plot the three mean values of λ averaged over the hyperbolic points directly imposed by the EM forcing. These mean values are, respectively, denoted $\lambda_3 = \lambda_{M10}$, $\lambda_2 = \lambda_{M40}$, and $\lambda_1 = \lambda_{M160}$, and correspond to length-scales M_{10}, M_{40}, and M_{160} which themselves correspond to the characteristic stagnation point scales L_s denoted L_{s_3}, L_{s_2}, L_{s_1}, respectively. In Fig. 3, λ_3, λ_2, and λ_1 are normalized by $u_{\rm rms}/L_E$ and are plotted against Re_{2D}. We observe that a clear multiscale structure appears for $\mathrm{Re}_{2D} \geq 5900$ when these stagnation point average strain rates clearly separate and the following dependence on their length scales is observed:

$$\frac{\lambda_i}{\lambda_{i+1}} \sim \left(\frac{L_{s_i}}{L_{s_{i+1}}}\right)^{-\alpha} \tag{1}$$

where α lies between 0.31 and 0.51 for the various values of Re_{2D} above 5900. In fact, there is a tendency for α to decrease with increasing Re_{2D}. As shown in Rossi *et al.* [13], the energy spectra of the multiscale flows used here are continuous and scale as $E(k) \sim k^{-p}$ with $p = 2.5$. The value of α consistent with $p = 2.5$ is $\alpha = 0.25$ for a $k^2E(k)$ strain-rate spectrum.

In the vicinity of a steady hyperbolic stagnation point, fluid element pairs of initial separation Δ_0 separate exponentially, i.e., $\Delta(t) \sim \Delta_0 e^{\lambda t}$. To complete the characterization of our multiscale stagnation point structure, we estimate the extent of this vicinity, i.e., the area of direct influence of each hyperbolic stagnation point. We define this area of influence as the region around $\mathbf{x}_s$ where the velocity field depends linearly on distance from $\mathbf{x}_s$. In suitable eigenframe coordinates, this is the area where $\mathbf{u} \approx \mathbf{u}_s \equiv [\lambda(x - x_s), -\lambda(y - y_s)]$. To quantify this area we calculate $\mathrm{Corr} \equiv \frac{\mathbf{u}\cdot\mathbf{u}_s}{\max(\mathbf{u}^2, \mathbf{u}_s^2)}$. This quantity Corr is found to fluctuate around a constant value close to or not much smaller than 1 in an area surrounding $\mathbf{x}_s$. Immediately beyond this area, Corr drops off very steeply. This is the area which we interpret as being the area of direct influence of the hyperbolic stagnation point and we plot it in Fig. 3 for the M_{160} hyperbolic stagnation point and for each of the four M_{40} hyperbolic stagnation points at four different Re_{2D} values.

Particle dispersion.—The Lagrangian trajectories $\frac{d}{dt}\mathbf{x}(t, \mathbf{x}_0) = \mathbf{u_L}(\mathbf{t}, \mathbf{x}_0) = \mathbf{u}(\mathbf{x}(\mathbf{t}, \mathbf{x}_0), \mathbf{t})$ and their statistics are calculated starting from random initial positions $\mathbf{x}_0$ at a time $t = 0$ well after the initial transient caused by the sudden switch-on of the electric field. These trajectories are integrated until $t = 4L_E/u_{\rm rms}$, and we extract statistics of fluid element pair separations $\Delta(t)$, specifically $\overline{\Delta^m}(t)$ for $m = 2, 3, 4, 5, 6$, the averages being carried out over many pairs of fluid elements (more than 10^6).

Pair statistics are initialized with initial separations $\Delta_0 = 1$ pixel which is about 25 times smaller than the size of the smallest magnet and therefore smaller than all the length scales of the flow by the size of the smallest magnets. Statistics such as mean square pair separations are sensitive to the choice of Δ_0 but the turbulent diffusivity $\frac{d}{dt}\overline{\Delta^2}$ is much less sensitive as shown recently in Ref. [7]. In addition, $\frac{d}{dt}\overline{\Delta^2}$ allows us to clearly identify different dispersion regimes such as the expected initial ballistic dispersion $\overline{\Delta^2} \sim t^2$, the final Brownian dispersion $\overline{\Delta^2} \sim t$ (see Ref. [13]) and a nontrivial Richardson-like regime in an intermediate range of times between the ballistic and the Brownian regimes.

Mean square pair separations are plotted in Figs. 4(a) and 5(b) and obey approximate power laws $\overline{\Delta^2} \sim t^\gamma$ for about one decade in time (Re_{2D} large enough). The exponents γ lie roughly between 2 and 3.

In our steady Q2D laminar flows, any mechanism leading to algebraic separation rates with values of γ larger than 2 must necessarily be rooted in the flows's multiscale stagnation point structure. However, pairs at the vicinity of straining stagnation points separate exponentially. Our measurements of $\partial\overline{\Delta^m}/\partial t$ for $m = 2, 3, 4, 5, 6$ exhibit oscillations in time, which appear weak for $m = 2$ (particularly at $\mathrm{Re}_{2D} = 7400$ where they hardly appear at all) but are progressively more pronounced as m is made larger; see Fig. 4. These oscillations can be interpreted as resulting from a sequence of exponential separations $\partial\overline{\Delta^m}/\partial t \propto e^{\beta_m^{(i)} t}$ where $i = 3, 2, 1$ label exponentials in a

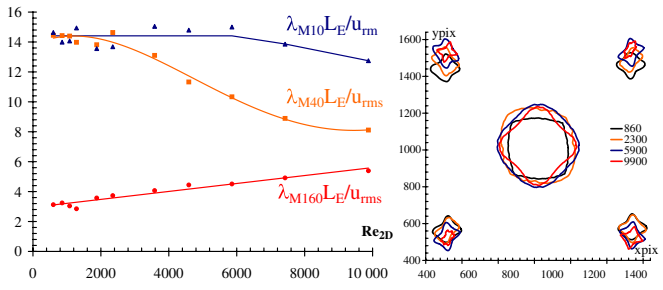

FIG. 3 (color online). Left: Dimensionless mean stagnation point strain rates versus Re_{2D}. Right: Areas of direct influence of stagnation points related to M_{160} and M_{40} for various Re_{2D}.

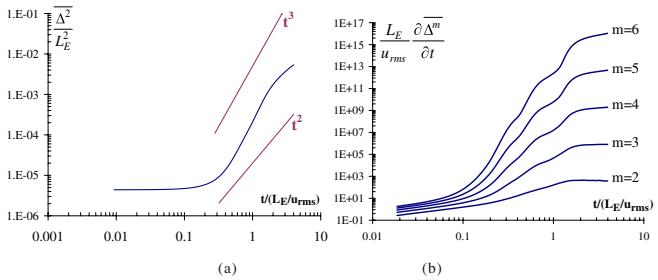

FIG. 4 (color online). Two-particle dispersion, $\mathrm{Re}_{2D} = 7400$, (a) $\overline{\Delta^2}/L_E^2$ (b) $\frac{L_E}{u_{\rm rms}}\frac{\partial\overline{\Delta^m}}{\partial t}$.

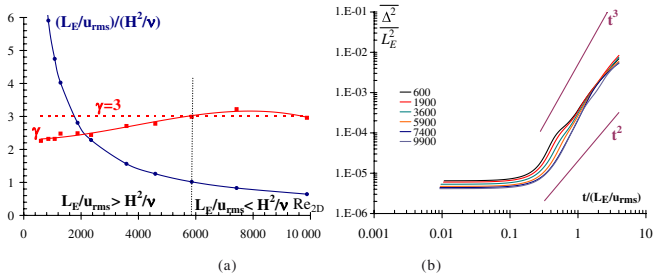

FIG. 5 (color online). (a) Richardson-like exponent, γ, ($\overline{\Delta^2} \sim t^\gamma$) and ratio $L_E/u_{\rm rms}$ to H^2/ν as function of Re_{2D}; (b) two-particle dispersion, $\overline{\Delta^2}/L_E^2$, various Re_{2D}.

sequence of three. Indeed, we find that such a sequence of exponentials fits the data well for all values of Re_{2D}. $\beta_m^{(3)}$, $\beta_m^{(2)}$, and $\beta_m^{(1)}$ are well-defined for all m in the respective time ranges 0 to $4/\lambda_3$, $(5-2)/\lambda_2$ to $5/\lambda_2$, and $(8-2)/\lambda_1$ to $8/\lambda_1$. This sequence of exponentials is further corroborated by the finding that (for all Re_{2D}) $\beta_m^{(i)} = m\lambda_{\Delta i}$ where $\lambda_{\Delta i}$ are comparable to the average stagnation point strain rates λ_i. Specifically, $\lambda_{\Delta 3}/\lambda_3$ is about 1, $\lambda_{\Delta 2}/\lambda_2$ is about 0.8, $\lambda_{\Delta 1}/\lambda_1$ is about 0.4, with standard deviation 0.1 across Reynolds numbers.

These findings suggest that, over the entire range of Reynolds numbers, pairs separate on average as a result of successive exponential straining actions by the stagnation points directly imposed by the three scales of EM forcing. The fact that the exponential separation rates appear in sequence with exponents closely related to the average stagnation point strain rates λ_i suggests a Richardson-like locality. The pair separation rate is first imposed by the ''smallest'' straining stagnation points corresponding to L_{s3}, then by the intermediate straining stagnation points corresponding to L_{s2} and finally by the ''largest'' stagnation point which corresponds to L_{s1}. Hence, the multiscale stagnation point structure of our flows drives pair diffusion in a Richardson-like manner. The oscillations superimposed on this behavior are weaker as Re_{2D} increases because the multiscale nature of distinct and ordered strain rates are better defined (see model calculation in Ref. [13] where it is shown that a succession of exponentials can give rise to power-law growth).

In the light of these results and conclusions we do not claim that $\overline{\Delta^2}$ has an exact power-law dependence on time. However, as argued in Refs. [5,13], a statistical sequence of exponential separation events (where pairs stay together for long and then suddenly separate) can integrate into an approximate power-law time dependence of $\overline{\Delta^2}$. Indeed, the data are well fitted by $\overline{\Delta^2} \sim t^\gamma$ over nearly a decade of times bounded from above by $2L_E/u_{\rm rms}$. The values of γ are given in Fig. 5 as function of Re_{2D}. They are extracted from best power-law fits of $\frac{d}{dt}\overline{\Delta^2}$ over the range $0.2 \leq tu_{\rm rms}/L_E \leq 2$.

The values of γ are found to increase with Re_{2D} while the topology of the flow does not change significantly: there is no increase in the number of stagnation points nor a systematic increase of the stagnation points's area of influence (Fig. 3). This increase of γ toward an approximately constant value beyond $\mathrm{Re}_{2D} \approx 5900$ is correlated with a steep decrease of the ratio of the large-scale turnover time, $L_E/u_{\rm rms}$, to the bottom friction's viscous time, H^2/ν (see Fig. 5). This ratio reaches 1 at $\mathrm{Re}_{2D} \approx 5900$ and is smaller for larger values of Re_{2D}. Hence, the Re_{2D} independent value of γ is reached once the bottom friction has been overcome by the EM forcing.

Conclusion.—It is perhaps an amusing coincidence that this asymptotic value of γ is close to 3, which is the value predicted for and observed in isotropic homogeneous turbulence [3,8–10]. It is nevertheless striking that our pair separation statistics exhibit Richardson-like locality and $\overline{\Delta^2} \sim t^\gamma$ with $\gamma \approx 3$ even though our flows are laminar, steady and Q2D. As shown, a power-law multiscale distribution of stagnation point strain rates is fully achieved only when $\mathrm{Re}_{2D} \geq 5900$ which perfectly corresponds with the onset of a constant γ value close to 3 and a bottom friction that has been overcome by the EM force field. Only at such high values of Re_{2D} are the stagnation point strain rates clearly distinct and ordered by stagnation point length scales (themselves ordered in approximate proportion to magnet sizes irrespective of Re_{2D}) according to (1). Note that the variations in γ are correlated with redistributions of the three stagnation point strain rates relative to each other (Fig. 3). We observe a maximum γ of about 3.2 ($\mathrm{Re}_{2D} = 7400$) in the case where (1) fits the data best.

Funding by the Leverhulme Trust, Royal Society, EPSRC.

[1] L. F. Richardson, Proc. R. Soc. A **110**, 709 (1926).
[2] J. C. H. Fung, J. C. R. Hunt, N. A. Malik, and R. J. Perkins, J. Fluid Mech. **236**, 281 (1992).
[3] M. C. Jullien, J. Paret, and P. Tabeling, Phys. Rev. Lett. **82**, 2872 (1999).
[4] J. C. H. Fung and J. C. Vassilicos, Phys. Rev. E **57**, 1677 (1998).
[5] S. Goto and J. C. Vassilicos, New J. Phys. **6**, 65 (2004).
[6] J. Davila and J. C. Vassilicos, Phys. Rev. Lett. **91**, 144501 (2003).
[7] F. Nicolleau and G. Yu, Phys. Fluids **16**, 2309 (2004).
[8] S. Ott and J. Mann, J. Fluid Mech. **422**, 207 (2000).
[9] G. Boffetta and I. M. Sokolov, Phys. Rev. Lett. **88**, 094501 (2002).
[10] T. Ishihara and Y. Kaneda, Phys. Fluids **14**, L69 (2002).
[11] S. Goto, D. R. Osborne, J. C. Vassilicos, and J. D. Haigh, Phys. Rev. E **71**, 015301 (2005).
[12] D. R. Osborne, J. C. Vassilicos, K.-S. Sung, J. D. Haigh, Phys. Rev. E **74**, 036309 (2006).
[13] L. Rossi, J. C. Vassilicos, and Y. Hardalupas, J. Fluid Mech. **558**, 207 (2006).
[14] J. M. Ottino, *The Kinematics of Mixing* (Cambridge University Press, Cambridge, England, 1989).